Age-Invariant Face Recognition

Article *in* IEEE Transactions on Pattern Analysis and Machine Intelligence · May 2010

DOI: 10.1109/TPAMI.2010.14 · Source: PubMed

3 authors, including:

Unsang Park
Sogang University
58 PUBLICATIONS **2,987** CITATIONS

SEE PROFILE

Yiying Tong
Michigan State University
126 PUBLICATIONS **6,278** CITATIONS

SEE PROFILE

Age-Invariant Face Recognition

Unsang Park, *Member*, *IEEE*,
Yiying Tong, *Member*, *IEEE*, and
Anil K. Jain, *Fellow*, *IEEE*

Abstract—One of the challenges in automatic face recognition is to achieve temporal invariance. In other words, the goal is to come up with a representation and matching scheme that is robust to changes due to facial aging. Facial aging is a complex process that affects both the 3D shape of the face and its texture (e.g., wrinkles). These shape and texture changes degrade the performance of automatic face recognition systems. However, facial aging has not received substantial attention compared to other facial variations due to pose, lighting, and expression. We propose a 3D aging modeling technique and show how it can be used to compensate for the age variations to improve the face recognition performance. The aging modeling technique adapts view-invariant 3D face models to the given 2D face aging database. The proposed approach is evaluated on three different databases (i.e., FG-NET, MORPH, and BROWNS) using FaceVACS, a state-of-the-art commercial face recognition engine.

Index Terms—Face recognition, facial aging, aging modeling, aging simulation, 3D face model.

1 Introduction

Face recognition accuracy is usually limited by large intraclass variations caused by factors such as pose, lighting, expression, and age [2]. Therefore, most of the current work on face recognition is focused on compensating for the variations that degrade face recognition performance. However, facial aging has not received adequate attention compared with other sources of variations such as pose, lighting, and expression.

Facial aging is a complex process that affects both the shape and texture (e.g., skin tone or wrinkles) of a face. This aging process also appears in different manifestations in different age groups. While facial aging is mostly represented by facial growth in younger age groups (e.g., ≤ 18 years old), it is mostly represented by relatively large texture changes and minor shape changes (e.g., due to change of weight or stiffness of skin) in older age groups (e.g., >18). Therefore, an age correction scheme needs to be able to compensate for both types of aging processes.

Some of the face recognition applications where age compensation is required include 1) identifying missing children, 2) screening, and 3) multiple enrollment detection problems. These three scenarios have two common characteristics: 1) significant age difference between probe and gallery images (images obtained at enrollment and verification stages) and 2) inability to obtain a user's face image to update the template (gallery).

Ling et al. [8] studied how age differences affect the face recognition performance in a real passport photo verification task. Their results show that the aging process does increase the recognition difficulty, but it does not surpass the effects of illumination or expression. Studies on face verification across age progression [9] have shown that: 1) Simulation of shape and texture variations caused by aging is a challenging task as factors like lifestyle and environment also contribute to facial changes in addition to biological factors, 2) the aging effects can be best understood using 3D scans of human head, and 3) the available databases to study facial aging are not only small but also contain uncontrolled external and internal variations. It is due to these reasons that the effect of aging in facial recognition has not been as extensively investigated as other factors that lead to intraclass variations in facial appearance.

Some biological and cognitive studies on aging process have also been conducted, e.g., in [10], [11]. These studies have shown that cardioidal strain is a major factor in the aging of facial outlines. Such results have also been used in psychological studies, e.g., by introducing aging as caricatures generated by controlling 3D model parameters [12]. A few seminal studies [3], [13] have demonstrated the feasibility of improving face recognition accuracy by simulated aging. There has also been some work done in the related area of age estimation using statistical models, e.g., [4], [14]. Geng et al. [5] learn a subspace of aging pattern based on the assumption that similar faces age in similar ways. Their face representation is composed of face texture and the 2D shape represented by the coordinates of the feature points as in the Active Appearance Models. Computer graphics community has also shown facial aging modeling methods in 3D domain [15], but the effectiveness of the aging model is not usually evaluated by conducting face recognition test.

Table 1 gives a brief comparison of various methods for modeling aging proposed in the literature. The performance of these models is evaluated in terms of the improvement in the identification accuracy. The identification accuracies of various studies in Table 1 cannot be directly compared due to the differences in the database, number of subjects, and the underlying face recognition method used for evaluation. Usually, the larger the number of subjects and the larger the database variations in terms of age, pose, lighting, and expression is, the smaller the recognition performance improvement due to aging model.

Compared with the other published approaches, the proposed method for aging modeling has the following features:

- 3D aging modeling: We use a pose correction stage and model the aging pattern more realistically in the *3D domain*. Considering that the aging is a 3D process, 3D modeling is better suited to capture the aging patterns. We have shown how to build a 3D aging model given a 2D face aging database. The proposed method is our only viable alternative to building a 3D aging model directly as no 3D aging database is currently available.
- Separate modeling of shape and texture changes: We have compared three different modeling methods, namely, shape modeling only, separate shape and texture modeling, and combined shape and texture modeling (e.g., applying second level PCA to remove the correlation between shape and texture after concatenating the two types of feature vectors). We have shown that the separate modeling is better than combined modeling method, given the FG-NET database as the training data.
- Evaluation using a state-of-the-art commercial face matcher, FaceVACS: All of the previous studies on facial aging have used PCA-based matchers. We have used a state-of-the-art face matcher, FaceVACS from Cognitec [16], to evaluate our aging model. The proposed method can thus be useful in practical applications requiring age correction process. Even though we have evaluated the proposed method only on one particular face matcher, it can be used directly in conjunction with any other 2D face matcher.
- Diverse Databases: We have used FG-NET for aging modeling and evaluated the aging model on three different databases, FG-NET (in leave-one-person-out fashion),

• *The authors are with the Department of Computer Science and Engineering, Michigan State University, 3105 Engineering Building, East Lansing, MI 48824. E-mail: {parkunsa, ytong, jain}@cse.msu.edu.*

Manuscript received 28 Oct. 2008; revised 10 Feb. 2009; accepted 25 July 2009; published online 7 Jan. 2010.
Recommended for acceptance by S. Li.
For information on obtaining reprints of this article, please send e-mail to: tpami@computer.org, and reference IEEECS Log Number TPAMI-2008-10-0745.
Digital Object Identifier no. 10.1109/TPAMI.2010.14.

TABLE 1
A Comparison of Methods Modeling Aging for Face Recognition

	Approach	Face matcher	Database (#subjects, #images) in probe and gallery	Rank-1 identification. accuracy (%)	
				original image	after aging model
Ramanathan et al. (2006) [3]	Shape growth modeling up to age 18	PCA	Private database (109,109)	8.0	15.0
Lanitis et al. (2002) [4]	Build an aging function in terms of PCA coefficients of shape and texture	Mahalanobis distance, PCA	Private database (12,85)	57.0	68.5
Geng et al. (2007) [5]	Learn aging pattern on concatenated PCA coefficients of shape and texture across a series of ages	Mahalanobis distance, PCA	FG-NET * (10,10)	14.4	38.1
Wang et al. (2006) [6]	Build an aging function in terms of PCA coefficients of shape and texture	PCA	Private database (NA,2000)	52.0	63.0
Patterson et al. (2006) [7]	Build an aging function in terms of PCA coefficients of shape and texture	PCA	MORPH + (9,36)	11.0	33.0
Proposed method	Learn aging pattern based on PCA coefficients in separated 3D shape and texture given 2D database	FaceVACS	FG-NET ** (82,82)	26.4	37.4
			MORPH-Album1 ++ (612,612)	57.8	66.4
			BROWNS (4,4) - probe (100,100) - gallery	15.6	28.1

* Used only a very small subset of the FG-NET database that contains 82 subjects
+ Used only a very small subset of the MORPH database that contains 625 subjects
** Used all the subjects of FG-NET
++ Used all the subjects in MORPH-Album1 which have multiple images

MORPH, and BROWNS. We have observed substantial performance improvements on all the three databases. This demonstrates the effectiveness of the proposed aging modeling method.

The rest of this paper is organized as follows: Section 2 introduces the preprocessing step of converting 2D images to 3D models, Section 3 describes our aging model, Section 4 presents the aging simulation methods using the aging model, and Section 5 provides experimental results and discussions. Section 6 summarizes our contributions and lists some directions for future work.

2 Converting 2D Images to 3D Models

We propose to use a set of 3D face models to learn the model for recognition, because the true craniofacial aging model [11] can be appropriately formulated only in 3D. However, since only 2D aging databases are available, it is necessary to first convert these 2D face images into 3D. We first define major notations that are used in the following sections:

- $\mathbf{S}_{mm} = \{S_{mm,1}, S_{mm,2}, \ldots, S_{mm,n_{mm}}\}$: a set of 3d face models used in constructing the reduced morphable model.
- $\mathbf{S}_\alpha$: reduced morphable model represented with model parameter α.
- $\mathbf{S}_{2d,i}^j = \{x_1, y_1, \ldots, x_{n_{2d}}, y_{n_{2d}}\}$: 2D facial feature points for the ith subject at age j. n_{2d} is the number of points in 2D.
- $\mathbf{S}_i^j = \{x_1, y_1, z_1, \ldots, x_{n_{3d}}, y_{n_{3d}}, z_{n_{3d}}\}$: 3D feature points for the ith subject at age j. n_{3d} is the number of points in 3D.
- $\mathbf{T}_i^j$: facial texture for ith subject at age j.
- $\mathbf{s}_i^j$: reduced shape of $\mathbf{S}_i^j$ after applying PCA on $\mathbf{S}_i^j$.
- $\mathbf{t}_i^j$: reduced texture of $\mathbf{T}_i^j$ after applying PCA on $\mathbf{T}_i^j$.
- $\mathbf{V}_s$: top L_s principle components of $\mathbf{S}_i^j$.
- $\mathbf{V}_t$: top L_t principle components of $\mathbf{T}_i^j$.
- $\mathbf{S}_{w_s}^j$: synthesized 3D facial feature points at age j represented with weight w_s.
- $\mathbf{T}_{w_t}^j$: synthesized texture at age j represented with weight w_t.
- $n_{mm} = 100$, $n_{2d} = 68$, $n_{3d} = 81$, $L_s = 20$, and $L_t = 180$.

In the following sections, we first transform $\mathbf{S}_{2d,i}^j$ to $\mathbf{S}_i^j$ using the reduced morphable model $\mathbf{S}_\alpha$. Then, 3D shape aging pattern space $\{\mathbf{S}_{w_s}\}$ and texture aging pattern space $\{\mathbf{T}_{w_t}\}$ are constructed using $\mathbf{S}_i^j$ and $\mathbf{T}_i^j$.

2.1 2D Facial Feature Point Detection

We use manually marked feature points in aging model construction. However, in the test stage, we need to detect the feature points automatically. The feature points on 2D face images are detected using the conventional Active Appearance Model (AAM) [17], [18].

2.2 3D Model Fitting

We use a simplified deformable model based on Blanz and Vetter's model [19]. For efficiency, we drastically reduced the number of vertices in the 3D morphable model to 81, 68 of which correspond to salient features present in the FG-NET database,

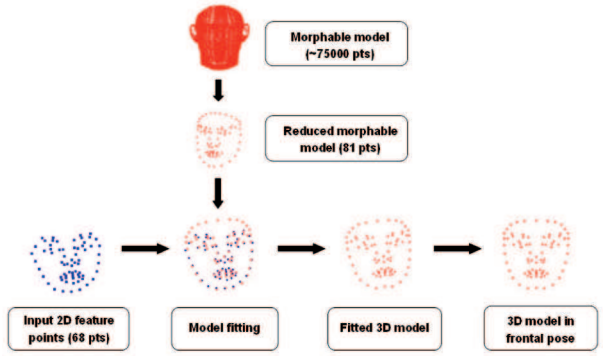

Fig. 1. 3D model fitting process using reduced morphable model.

while the other 13 delineate the forehead region. Following [19], we perform PCA on the simplified shape sample set, $\{S_{mm}\}$. We obtain the mean shape $\overline{\mathbf{S}}_{mm}$, the eigenvalues λ_ls, and unit eigenvectors $\mathbf{W}_l$s of the shape covariance matrix. We use only the top L $(= 30)$ eigenvectors, again for efficiency and stability of the subsequent fitting algorithm performed on the possibly very noisy data sets. A 3D face shape can then be represented using the eigenvectors as

$$\mathbf{S}_\alpha = \overline{\mathbf{S}}_{mm} + \sum_{l=1}^{L} \alpha_l \mathbf{W}_l, \tag{1}$$

where the parameter $\alpha = [\alpha_l]$ controls the shape and the covariance of αs is the diagonal matrix with λ_i as the diagonal elements. We now describe how to transform the given 2D feature points $\mathbf{S}^j_{2d,i}$ to the corresponding 3D points $\mathbf{S}^j_i$ using the reduced morphable model $\mathbf{S}_\alpha$.

Let $E(\cdot)$ be the overall error in fitting the 3D model of one face to its corresponding 2D feature points, where

$$E(\mathbf{P}, \mathbf{R}, \mathbf{t}, a, \{\alpha_l\}_{l=1}^{L}) = \left\| \mathbf{S}^j_{i,2d} - \mathbf{T}_{\mathbf{P},\mathbf{R},\mathbf{t},a}(\mathbf{S}_\alpha) \right\|^2. \tag{2}$$

Here $\mathbf{T}(\cdot)$ represents a transformation operator performing a sequence of operations, i.e., rotation, translation, scaling, projection, and selecting n_{2d} points out of n_{3d} that have correspondences. To simplify the procedure, an orthogonal projection $\mathbf{P}$ is used.

In practice, the 2D feature points that are either manually labeled or generated by AAM are noisy, which means overfitting these feature points may produce undesirable 3D shapes. We address this issue by introducing a Tikhonov regularization term to control the Mahalanobis distance of the shape from the mean shape. Let σ be the empirically estimated standard deviation of the energy E induced by the noise in the location of the 2D feature points. We define our regularized energy as

$$E' = E/\sigma^2 + \sum_{l=1}^{L} \alpha_l^2/\lambda_l. \tag{3}$$

To minimize the energy term defined in (3), we initialize all of the α_ls to 0, set the rotation matrix $\mathbf{R}$ to the identity matrix and translation vector $\mathbf{t}$ to 0, and set the scaling factor a to match the overall size of the 2D and 3D shapes. Then, we iteratively update $\mathbf{R}$, $\mathbf{T}$, and α until convergence. There are multiple ways to find the optimal pose given the current α. In our tests, we found that first estimating best 2×3 affine transformation followed by a QR decomposition to get the rotation works better than running a quaternion-based optimization using Rodriguez's formula [20]. Note that $\mathbf{t}_z$ is fixed to 0 as we use an orthogonal projection.

Fig. 1 illustrates the 3D model fitting process to acquire the 3D shape. The associated texture is then retrieved by warping the 2D image.

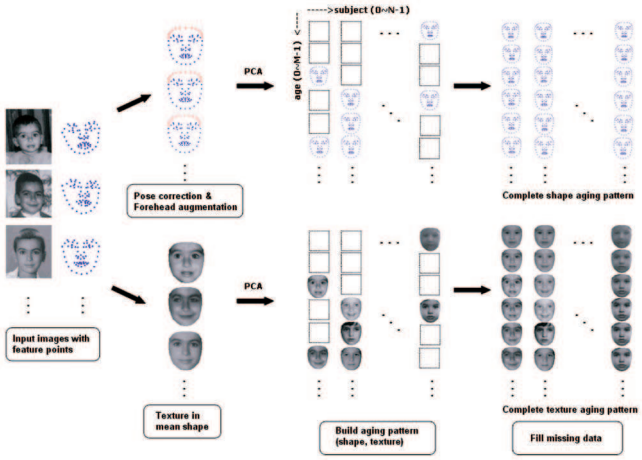

Fig. 2. 3D aging model construction.

3 3D Aging Model

Following [5], we define the aging pattern as an array of face models from a single subject indexed by her age. We assume that any aging pattern can be approximated by a weighted average of the aging patterns in the training set. Our model construction differs from [5] mainly in that we model shape and texture separately at different ages using the shape (aging) pattern space and the texture (aging) pattern space, respectively, because the 3D shape and the texture images are less correlated than the 2D shape and texture that they use. We also adjust the 3D shape as explained below. The two pattern spaces are described below.

3.1 Shape Aging Pattern

Shape pattern space captures the variations in the internal shape changes and the size of the face. The pose-corrected 3D models obtained from the preprocessing phase are used for constructing the shape pattern space. Under age 19, the key effects of aging are driven by the increase in the cranial size, while, at later ages, the facial growth in height and width is very small [21]. To incorporate the growth pattern of the cranium for ages under 19, we rescale the overall size of 3D shapes according to the average anthropometric head width found in [22].

We perform PCA over all the 3D shapes, $\mathbf{S}^j_i$, in the database irrespective of age j and subject i. We project all the mean subtracted $\mathbf{S}^j_i$ onto the subspace spanned by the columns of $\mathbf{V}_s$ to obtain $\mathbf{s}^j_i$ as

$$\mathbf{s}^j_i = \mathbf{V_s}^T (\mathbf{S}^j_i - \overline{\mathbf{S}}), \tag{4}$$

which is an $L_s \times 1$ vector.

Assuming that we have n subjects at m ages, the basis of the shape pattern space is then assembled as an $m \times n$ matrix with vector entries (or, alternatively, as an $m \times n \times L_s$ tensor), where the jth row corresponds to age j and the ith column corresponds to subject i, and the entry at (j, i) is $\mathbf{s}^j_i$. The shape pattern basis is initialized with the projected shapes $\mathbf{s}^j_i$ from the face database (as shown in the third column of Fig. 2). Then, we fill missing values using the available values along the same column (i.e., for the same subject). We tested three different methods for the filling process: linear, Radial Basis Function (RBF), and a variant of RBF (v-RBF). Given available ages a_i and the corresponding shape feature vectors s_i, a missing feature value s_x at age a_x can be estimated by $s_x = l_1 \times s_1 + l_2 \times s_2$ in linear interpolation, where s_1 and s_2 are shape features corresponding to the ages a_1 and a_2 that are closest from a_x and l_1 and l_2 are weights inversely proportionate to the distance from a_x to a_1 and a_2. In the v-RBF process, each feature is replaced by a weighted sum of all

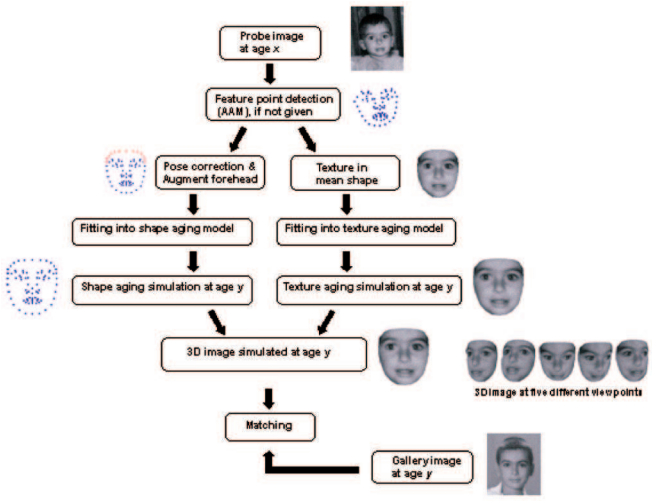

Fig. 3. Aging simulation from age x to y.

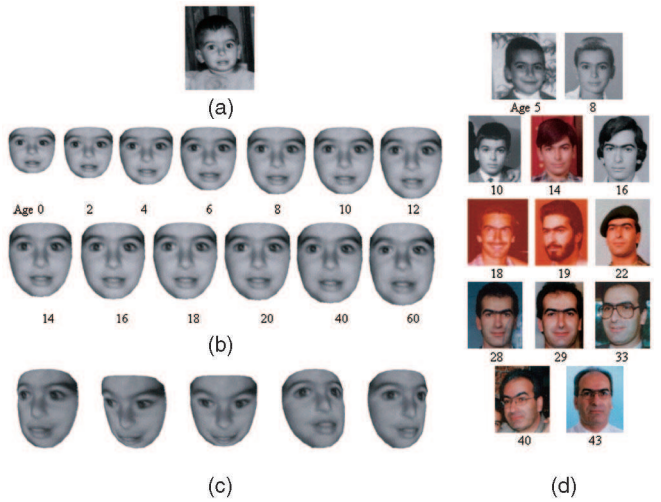

Fig. 4. Example aging simulation in FG-NET database. (a) Given image at age 2. (b) Aging-simulated images from age 0 to 60. (c) Face images at five different poses from the aging-simulated image at age 20. (d) Ground truth images.

available features as $s_x = \sum_i \phi(a_x - a_i)s_i/(\sum \phi(a_x - a_i))$, where $\phi(.)$ is an RBF function defined by a Gaussian function. In the RBF method, the mapping function from age to shape feature vector is calculated by $s_x = \sum_i r_i\phi(a_x - a_i)/(\sum \phi(a_x - a_i))$ for each available age and feature vector a_i and s_i, where r_is are estimated based on the known scattered data. Any missing feature vector s_x at age x can thus be obtained.

The shape aging pattern space is defined as the space containing all linear combinations of the patterns of the following type (expressed in PCA basis):

$$\mathbf{s}^j_{w_s} = \overline{\mathbf{s}^j} + \sum_{i=1}^{n} \left(\mathbf{s}^j_i - \overline{\mathbf{s}^j}\right) w_{s,i}, \quad 0 \le j \le m-1. \tag{5}$$

Note that the weight w_s in the linear combination above is not unique for the same aging pattern. We can use the regularization term in the aging simulation described below to resolve this issue. Given a complete shape pattern space, mean shape $\overline{\mathbf{S}}$ and the transformation matrix $\mathbf{V_s}$, the shape aging model with weight w_s is defined as

$$\mathbf{S}^j_{w_s} = \overline{\mathbf{S}} + \mathbf{V_s}\mathbf{s}^j_{w_s}, \quad 0 \le j \le m-1. \tag{6}$$

3.2 Texture Aging Pattern

The texture pattern T^j_i for subject i at age j is obtained by mapping the original face image to frontal projection of the mean shape $\overline{\mathbf{S}}$ followed by column-wise concatenation of the image pixels. After applying PCA on T^j_i, we calculate the transformation matrix V_t and the projected texture t^j_i. We follow the same filling procedure as in the shape pattern space to construct the complete basis for the texture pattern space using t^j_i. A new texture $\mathbf{T}^j_{w_t}$ can be similarly obtained, given an age j and a set of weights w_t, as

$$\mathbf{t}^j_{w_t} = \overline{\mathbf{t}^j} + \sum_{i=1}^{n} \left(\mathbf{t}^j_i - \overline{\mathbf{t}^j}\right) w_{t,i}, \tag{7}$$

$$\mathbf{T}^j_{w_t} = \overline{\mathbf{T}} + \mathbf{V_t}\mathbf{t}^j_{w_t}, \; 0 \le j \le m-1. \tag{8}$$

Fig. 2 illustrates the aging model construction process for shape and texture pattern spaces.

4 Aging Simulation

Given a face image of a subject at a certain age, aging simulation involves the construction of the face image of that subject adjusted to a different age.

Given an image at age x, we first produce the 3D shape, $\mathbf{S}^x_{new}$, and the texture, T^x_{new}, by following the preprocessing step described in Section 2, and then project them to the reduced spaces to get $\mathbf{s}^x_{new}$ and $\mathbf{t}^x_{new}$. Given a reduced 3D shape $\mathbf{s}^x_{new}$ at age x, we can obtain a weighting vector, w_s, that generates the closest possible weighted sum of the shapes at age x as

$$\hat{w_s} = \underset{c_- \le w_s \le c_+}{\operatorname{argmin}} \left\|\mathbf{s}^x_{new} - \mathbf{s}^x_{w_s}\right\|^2 + r_s\|w_s\|^2, \tag{9}$$

where r_s is the weight of a regularizer to handle the cases when multiple solutions are obtained or when the linear system used to obtain the solution has a large condition number. We constrain each element of weight vector, $w_{s,i}$, within $[c_-, c_+]$ to avoid strong domination by a few shape basis vectors.

Given $\hat{w_s}$, we can obtain age-adjusted shape at age y by carrying $\hat{w_s}$ over to the shapes at age y and transforming the shape descriptor back to the original shape space as

$$S^y_{new} = \mathbf{S}^y_{\hat{w_s}} = \overline{\mathbf{S}} + \mathbf{V_s}\mathbf{s}^y_{\hat{w_s}}. \tag{10}$$

The texture simulation process is similarly performed by first estimating $\hat{w_t}$ as

$$\hat{w_t} = \underset{c_- \le w_t \le c_+}{\operatorname{argmin}} \left\|\mathbf{t}^x_{new} - \mathbf{t}^x_{w_t}\right\|^2 + r_t\|w_t\|^2, \tag{11}$$

and then propogating the $\hat{w_t}$ to the target age y followed by the back projection to get

$$T^y_{new} = \mathbf{T}^y_{\hat{w_t}} = \overline{\mathbf{T}} + \mathbf{V_t}\mathbf{t}^y_{\hat{w_t}}. \tag{12}$$

The aging simulation process is illustrated in Fig. 3. Fig. 4 shows an example of aging-simulated face images from a subject at age 2 in the FG-NET database. Fig. 5 exhibits the example input images, feature point detection, and pose-corrected and age-simulated images from a subject in the MORPH database.

5 Results and Discussion

5.1 Database

There are two well-known public domain databases to evaluate facial aging models: FG-NET [23] and MORPH [24]. The FG-NET database contains 1,002 face images of 82 subjects (~12 images/subject) at different ages, with the minimum age being 0 (<12 months) and the maximum age being 69. There are two

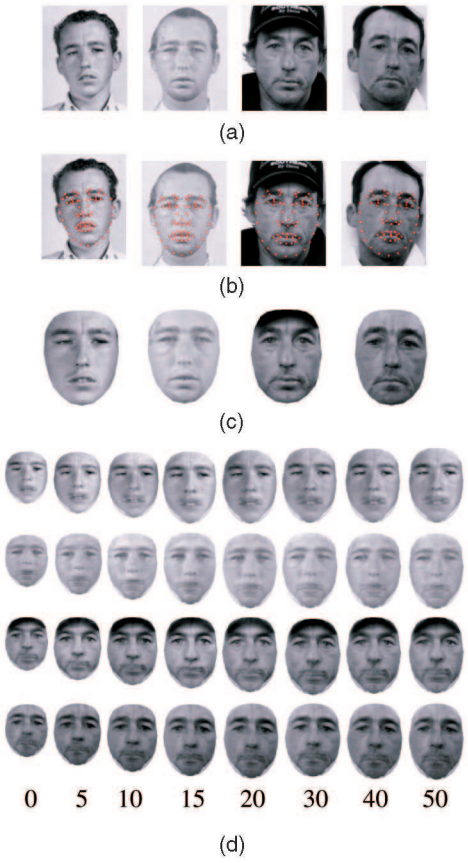

Fig. 5. Example aging simulation process in MORPH database. (a) Input images (ages 16, 25, 39, and 42 from the same subject). (b) Feature poing detection (AAM). (c) Pose correction. (d) Aging simulation at indicated ages for each of the four images in (a).

separate databases in MORPH: Album1 and Album2. MORPH-Album1 contains 1,690 images from 625 different subjects (~2.7 images/subject). MORHP-Album2 contains 15,204 images from 4,039 different subjects (~3.8 images/subject). Another source of facial aging data that we have used can be found in the book by Nixon and Galassi [25]. This is a collection of pictures of four sisters taken every year over a period of 33 years from 1975 to 2007. We have scanned 132 pictures of the four subjects (33 per subject) from the book and composed a new database, called, "BROWNS," to evaluate our proposed aging model. We have used the complete FG-NET database for model construction and evaluated it on FG-NET (in leave-one-person-out fashion), MORPH-Album1, and BROWNS.

5.2 Face Recognition Tests

We evaluate the performance of the proposed aging model by comparing the face recognition accuracy of a state-of-the-art matcher before and after aging simulation. We construct the probe set, $P = \{p_1^{x_1}, \ldots, p_n^{x_n}\}$, by selecting one image $p_i^{x_i}$ for each subject i at age x_i in each database, $i \in \{1, \ldots, n\}$, $x_i \in \{0, \ldots, m-1\}$. The gallery set $G = \{g_1^{y_1}, \ldots, g_n^{y_n}\}$ is similarly constructed. We also created a number of different probe and gallery age groups from the three databases to demonstrate our model's effectiveness in different periods of the aging process.

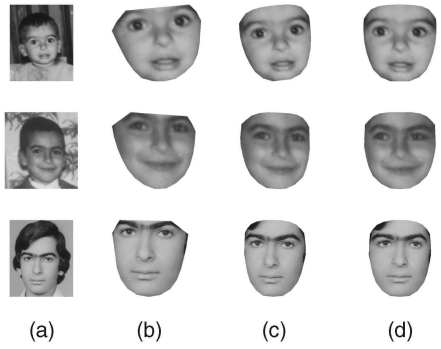

Fig. 6. Example images showing different face cropping methods: (a) original, (b) no-forehead and no pose correction, (c) no pose correction with forehead, (d) pose correction with forehead.

Aging simulation is performed in both aging and de-aging directions for each subject i in the probe and each subject j in the gallery as $(x_i \rightarrow y_j)$ and $(y_j \rightarrow x_i)$. Table 2 summarizes the probe and gallery data sets used in our face recognition test.

Let P, P_f, and P_a denote the probe, the pose-corrected probe, and the age-adjusted probe set, respectively. Let G, G_f, and G_a denote the gallery, the pose-corrected gallery, and age-adjusted gallery set, respectively. All age-adjusted images are generated (in leave-one-person-out fashion for FG-NET) using the shape and texture pattern space. The face recognition test is performed on the following probe-gallery pairs: P-G, P-G_f, P_f-G, P_f-G_f, P_a-G_f, and P_f-G_a. The identification rate for the probe-gallery pair P-G is the performance on original images without applying the aging model. The accuracy obtained by fusion of P-G, P-G_f, P_f-G, and P_f-G_f matchings is regarded as the performance after pose correction. The accuracy obtained by fusion of all the pairs P-G, P-G_f, P_f-G, P_f-G_f, P_a-G_f, and P_f-G_a represents the performance after aging simulation. A simple score-sum-based fusion is used in all the experiments.

5.3 Effects of Different Cropping Methods

We study the performance of the face recognition system with different face cropping methods. An illustration of the cropping results obtained by different approaches is shown in Fig. 6. The first column shows the input face image and the second column shows the cropped face obtained using the 68 feature points provided in the FG-NET database, without pose correction. The third column shows the cropped face obtained with the additional 13 points (total 81 feature points) for forehead inclusion, without any pose correction. The last column shows the cropping obtained by the 81 feature points, with pose correction.

TABLE 2
Probe and Gallery Data Used in Face Recognition Tests

Database	Probe			Gallery		
	#images	#subjects	age group	#images	#subjects	age group
FG-NET	82	82	$\{0, 5, \cdots, 30\}$	82	82	$x^* + \{5, 10, \cdots, 30\}$
MORPH	612	612	$\{15, 20, \cdots, 30\}$	612	612	$x + \{5, 10, \cdots, 30\}$
BROWNS	4	4	$\{15, 20, \cdots, 30\}$	100	100	$x + \{5, 10, \cdots, 30\}$

$*$ x is the age of the probe group

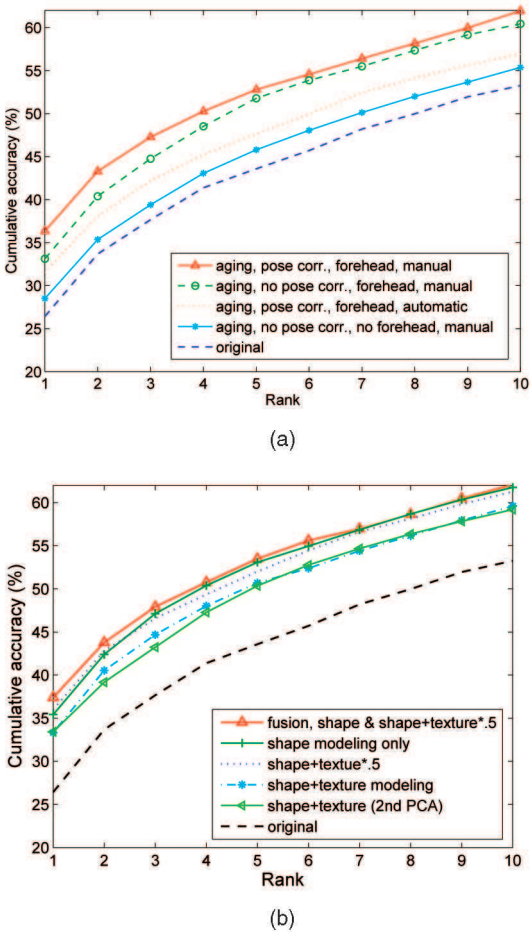

Fig. 7. Cumulative match characteristic (CMC) curves with different methods of face cropping and shape and texture modeling. (a) CMC with different methods of face cropping. (b) CMC with different methods of shape and texture modeling.

Fig. 7a shows the face recognition performance on FG-NET using only shape modeling based on different face cropping methods and feature point detection methods. Face images with pose correction that include the forehead show the best performance. This result shows that the forehead does influence the face recognition performance, although it has been a common practice to remove the forehead in AAM-based feature point detection and subsequent face modeling [4], [6], [18]. We therefore evaluate our aging simulation with the model that contains the forehead region with pose correction.

5.4 Effects of Different Strategies in Employing Shape and Texture

Most of the existing face aging modeling techniques use either only shape or a combination of shape and texture [3], [4], [5], [6], [7]. We have tested our aging model with shape only, separate shape and texture, and combined shape and texture modeling. In our test of the combined scheme, the shape and the texture are concatenated and a second stage of principle component analysis is applied to remove the possible correlation between shape and texture as in the AAM face modeling technique.

Fig. 7b shows the face recognition performance of different approaches to shape and texture modeling. We have observed consistent performance drop in face recognition performance when the texture is used together with the shape. The best performance is observed by combining shape modeling and $\text{shape} + \text{texture}$ modeling using score-level fusion. When simulating the texture, we have blended the aging-simulated texture and the original texture with equal weights. Unlike the shape, the texture is a higher dimensional vector that can easily deviate from its original identity after the aging simulation. Even though performing aging simulation on texture produces more realistic face images, it can easily lose the original face-based identity information. The blending process with the original texture reduces the deviation and generates better recognition performance. In Fig. 7b, $\text{shape} + \text{texture}$ modeling represents separate modeling of shape and texture, $\text{shape} + \text{texture} \times 0.5$ represents the same procedure but with the blending of the simulated texture with the original texture. We use the fusion of shape and $\text{shape} + \text{texture} \times 0.5$ strategy for the following aging modeling experiments.

5.5 Effects of Different Filling Methods in Model Construction

We tried a few different methods of filling missing values in aging pattern space construction (see Section 3.1): linear, v-RBF, and RBF. The rank-one accuracies are obtained as 36.12 percent, 35.19 percent, and 36.35 percent in $\text{shape} + \text{texture} \times 0.5$ modeling method for linear, v-RBF, and RBF methods, respectively. We chose the linear interpolation method in the rest of the experiments for the following reasons: 1) The difference is minor, 2) linear interpolation is computationally efficient, and 3) the calculation of RBF-based mapping function can be ill-posed.

Fig. 8 provides the Cumulative Match Characteristic (CMC) curves with original, pose-corrected and aging-simulated images in FG-NET, MORPH, and BROWNS, respectively. It can be seen that there are significant performance improvements after aging modeling and simulation in all the three databases. The order of improvement due to aging simulation is more or less similar with those of other studies as shown in Table 1. However, we have used FaceVACS, a state-of-the-art face matcher, which is known to be more robust against internal and external facial variations (e.g., pose, lighting, expression, etc.) than simple PCA-based matchers. We argue that the performance gain using FaceVACS is more

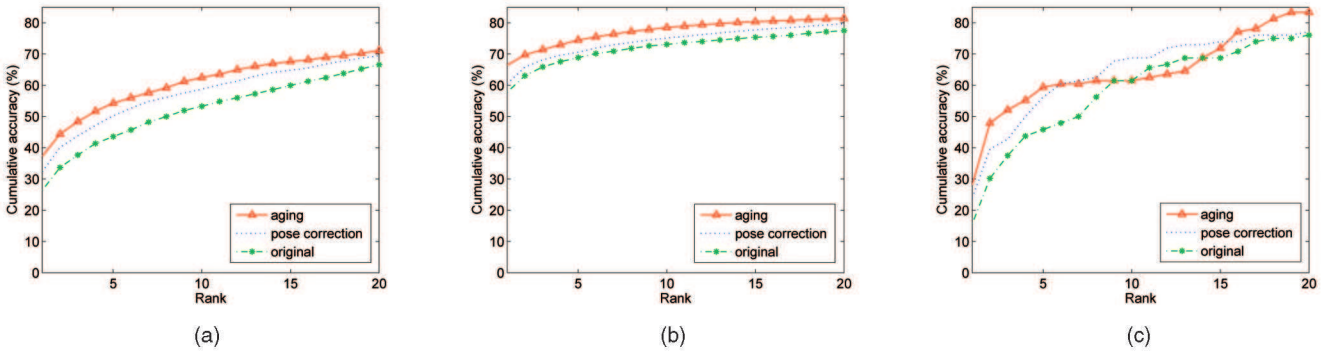

Fig. 8. Cumulative match characteristic (CMC) curves. (a) FG-NET. (b) MORPH. (c) BROWNS.

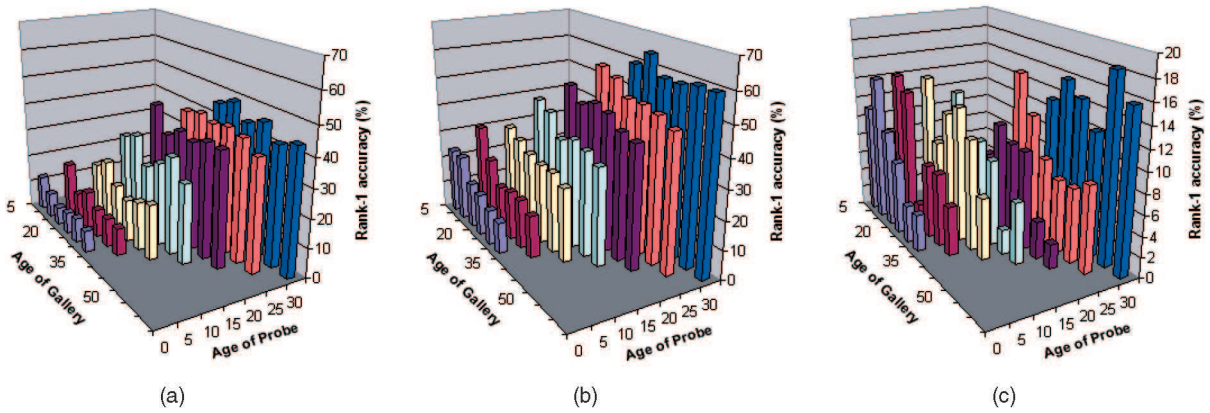

Fig. 9. Rank-one identification accuracies for each probe and gallery age groups: (a) before aging simulation, (b) after aging simulation, and (c) the amount of improvement after aging simulation.

realistic than that of a PCA matcher reported in other studies. Further, unlike other studies, we have used the entire FG-NET and MORPH-Album1 in our experiments. Another unique attribute of our studies is that the model is built on FG-NET and then evaluated on MORPH and BROWNS.

Fig. 10. Example matching results before and after aging simulation for seven different subjects: (a) probe, (b) pose-corrected probe, (c) age-adjusted probe, (d) pose-corrected gallery, and (e) gallery. All of the images in (b) failed to match with the corresponding images in (d), but images in (c) were successfully matched to the corresponding images in (d) for the first five subjects. Matching for the last two subjects failed both before and after aging simulation. The ages of (probe, gallery) pairs are (0,18), (0,9), (4,14), (3,20), (30,49), (0,7) and (23,31), respectively, from the top to bottom row.

Fig. 9 presents the rank-one identification accuracies for each of the 42 different age pair groups of probe and gallery in FG-NET database. The aging process can be separated as growth and development (age ≤ 18) and adult aging process (age > 18). The face recognition performance is somewhat lower in the growth process where more changes occurs in the facial appearance. However, our aging process provides performance improvements in both the age groups, ≤ 18 and >18. The average recognition results for age groups ≤ 18 are improved from 17.3 percent to 24.8 percent and those for age groups >18 are improved from 38.5 percent to 54.2 percent.

Matching results for seven subjects in FG-NET are demonstrated in Fig. 10. The face recognition fails without aging simulation but succeeds with aging simulations for the first five of the seven subjects. The aging simulation fails to provide correct matchings for the last two subjects, possibly due to poor texture quality (for the sixth subject) or large pose and illumination variation (for the seventh subject).

The proposed aging model construction takes about 44 seconds. The aging model is constructed offline; therefore, its computation time is not a major concern. In the recognition stage, the entire process, including feature points detection, aging simulation, enrollment, and matching takes about 12 seconds per probe image. Note that the gallery images are preprocessed offline. All computation times are measured on a Pentium 4, 3.2 GHz, 3GByte RAM machine.

6 Conclusion and Future Work

We have proposed a 3D facial aging model and simulation method for age-invariant face recognition. The extension of shape modeling from 2D to 3D domain gives additional capability of compensating for pose and, potentially, lighting variations. Moreover, we believe that the use of 3D model provides more powerful modeling capability than 2D age modeling proposed earlier because the change in human face configuration occurs in 3D domain. We have evaluated our approach using a state-of-the-art commercial face recognition engine (FaceVACS), and showed improvements in face recognition performance on three different publicly available aging databases. We have shown that our method is capable of handling both growth (developmental) and adult face aging effects.

Exploring different (nonlinear) methods for building aging pattern space given noisy 2D or 3D shape and texture data with cross validation of the aging pattern space and aging simulation results in terms of face recognition performance can further improve simulated aging. Age estimation is crucial if a fully automatic age-invariant face recognition system is needed.

ACKNOWLEDGMENTS

One of the authors (Anil K. Jain) is also affiliated with the World Class University Program in the Department of Brain and Cognitive Engineering at Korea University, Anam-dong, Seongbuk-ku, Seoul 136-701, Korea. An earlier version of this work appeared in the *Proceedings of the International Conference on Automatic Face and Gesture Recognition*, 2008 [1].

REFERENCES

[1] U. Park, Y. Tong, and A.K. Jain, "Face Recognition with Temporal Invariance: A 3D Aging Model," *Proc. Int'l Conf. Automatic Face and Gesture Recognition,* pp. 1-7, 2008.
[2] P.J. Phillips, W.T. Scruggs, A.J. O'Toole, P.J. Flynn, K.W. Bowyer, C.L. Schott, and M. Sharpe, "FRVT 2006 and ICE 2006 Large-Scale Results," Technical Report NISTIR 7408, Nat'l Inst. of Standards and Technology, Mar. 2007.
[3] N. Ramanathan and R. Chellappa, "Modeling Age Progression in Young Faces," *Proc. IEEE CS Conf. Computer Vision and Pattern Recognition,* vol. 1, pp. 387-394, 2006.
[4] A. Lanitis, C.J. Taylor, and T.F. Cootes, "Toward Automatic Simulation of Aging Effects on Face Images," *IEEE Trans. Pattern Analysis and Machine Intelligence,* vol. 24, no. 4, pp. 442-455, Apr. 2002.
[5] X. Geng, Z.-H. Zhou, and K. Smith-Miles, "Automatic Age Estimation Based on Facial Aging Patterns," *IEEE Trans. Pattern Analysis and Machine Intelligence,* vol. 29, no. 7, pp. 2234-2240, Dec. 2007.
[6] J. Wang, Y. Shang, G. Su, and X. Lin, "Age Simulation for Face Recognition," *Proc. Int'l Conf. Pattern Recognition,* pp. 913-916, 2006.
[7] E. Patterson, K. Ricanek, M. Albert, and E. Boone, "Automatic Representation of Adult Aging in Facial Images," *Proc. Int'l Conf. Visualization, Imaging, and Image Processing,* pp. 171-176, 2006.
[8] H. Ling, S. Soatto, N. Ramanathan, and D. Jacobs, "A Study of Face Recognition as People Age," *Proc. IEEE Int'l Conf. Computer Vision,* pp. 1-8, 2007.
[9] N. Ramanathan and R. Chellappa, "Face Verification Across Age Progression," *Proc. IEEE CS Conf. Computer Vision and Pattern Recognition,* vol. 2, pp. 462-469, 2005.
[10] D.W. Thompson, *On Growth and Form.* Dover Publications, 1992.
[11] J.B. Pittenger and R.E. Shaw, "Aging Faces as Viscal-Elastic Events: Implications for a Theory of Nonrigid Shape Perception," *J. Experimental Psychology: Human Perception and Performance,* vol. 1, pp. 374-382, 1975.
[12] A. O'Toole, T. Vetter, H. Volz, and E. Salter, "Three-Dimensional Caricatures of Human Heads: Distinctiveness and the Perception of Facial Age," *Perception,* vol. 26, pp. 719-732, 1997.
[13] J. Suo, F. Min, S. Zhu, S. Shan, and X. Chen, "A Multi-Resolution Dynamic Model for Face Aging Simulation," *Proc. IEEE CS Conf. Computer Vision and Pattern Recognition,* pp. 1-8, 2007.
[14] A. Lanitis, C. Draganova, and C. Christodoulou, "Comparing Different Classifiers for Automatic Age Estimation," *IEEE Trans. Systems, Man, and Cybernetics, Part B: Cybernetics,* vol. 34, no. 1, pp. 621-628, Feb. 2004.
[15] K. Scherbaum, M. Sunkel, H.-P. Seidel, and V. Blanz, "Prediction of Individual Non-Linear Aging Trajectories of Faces," *Computer Graphics Forum,* vol. 26, no. 3, pp. 285-294, 2007.
[16] "FaceVACS Software Developer Kit, Cognitec Systems GmbH," http://www.cognitec-systems.de, 2010.
[17] M.B. Stegmann, "The AAM-API: An Open Source Active Appearance Model Implementation," *Proc. Int'l Conf. Medical Image Computing and Computer-Assisted Intervention,* pp. 951-952, 2003.
[18] T.F. Cootes, G.J. Edwards, and C.J. Taylor, "Active Appearance Models," *IEEE Trans. Pattern Analysis and Machine Intelligence,* vol. 23, no. 6, pp. 681-685, June 2001.
[19] V. Blanz and T. Vetter, "A Morphable Model for the Synthesis of 3D Faces," *Proc. ACM SIGGRAPH Conf. Computer Graphics and Interactive Techniques,* pp. 187-194, 1999.
[20] F. Pighin, R. Szeliski, and D.H. Salesin, "Modeling and Animating Realistic Faces from Images," *Int'l J. Computer Vision,* vol. 50, no. 2, pp. 143-169, 2002.
[21] A. Albert, K. Ricanek, and E. Patterson, "The Aging Adult Skull and Face: A Review of the Literature and Report on Factors and Processes of Change," UNCW Technical Report WRG FSC-A, 2004.
[22] *Anthropometry of the Head and Face,* L.G. Farkas, ed. Lippincott Williams & Wilkins, 1994.
[23] "FG-NET Aging Database," http://www.fgnet.rsunit.com, 2010.
[24] K.J. Ricanek and T. Tesafaye, "Morph: A Longitudinal Image Database of Normal Adult Age-Progression," *Proc. Int'l Conf. Automatic Face and Gesture Recognition,* pp. 341-345, 2006.
[25] N. Nixon and P. Galassi, *The Brown Sisters, Thirty-Three Years.* The Museum of Modern Art, 2007.